Yong X. Chen
Department of Biomedical
and Chemical Engineering,
Syracuse University,
900 S. Crouse Avenue,
Syracuse, NY 13210
e-mail: ychen35@syr.edu

Shihao Yang
Department of Biomedical
and Chemical Engineering,
Syracuse University,
900 S. Crouse Avenue,
Syracuse, NY 13210
e-mail: syang21@syr.edu

Jiahan Yan
Department of Biomedical and Chemical
Engineering,
Syracuse University,
900 S. Crouse Avenue,
Syracuse, NY 13210
e-mail: jyan13@syr.edu

Ming-Han Hsieh
Department of Biomedical
and Chemical Engineering,
Syracuse University,
900 S. Crouse Avenue,
Syracuse, NY 13210
e-mail: mhsieh01@syr.edu

Lingyan Weng
Department of Biomedical
and Chemical Engineering,
Syracuse University,
900 S. Crouse Avenue,
Syracuse, NY 13210
e-mail: lweng@syr.edu

Jessica L. Ouderkirk
Department of Biomedical and Chemical
Engineering,
Syracuse University,
900 S. Crouse Avenue,
Syracuse, NY 13210
e-mail: jloude6@gmail.com

Mira Krendel
Department of Cell and Developmental Biology,
SUNY Upstate Medical University,
750 East Adams Street,
Syracuse, NY 13210
e-mail: krendelm@upstate.edu

Pranav Soman
Department of Biomedical and Chemical
Engineering,
Syracuse University,
900 S. Crouse Avenue,
Syracuse, NY 13210
e-mail: psoman@syr.edu

A Novel Suspended Hydrogel Membrane Platform for Cell Culture

Current cell-culture is largely performed on synthetic two-dimensional (2D) petri dishes or permeable supports such as Boyden chambers, mostly because of their ease of use and established protocols. It is generally accepted that modern cell biology research requires new physiologically relevant three-dimensional (3D) cell culture platform to mimic in vivo cell responses. To that end, we report the design and development of a suspended hydrogel membrane (ShyM) platform using gelatin methacrylate (GelMA) hydrogel. ShyM thickness (0.25–1 mm) and mechanical properties (10–70 kPa) can be varied by controlling the size of the supporting grid and concentration of GelMA prepolymer, respectively. GelMA ShyMs, with dual media exposure, were found to be compatible with both the cell-seeding and the cell-encapsulation approach as tested using murine 10T1/2 cells and demonstrated higher cellular spreading and proliferation as compared to flat GelMA unsuspended control. The utility of ShyM was also demonstrated using a case-study of invasion of cancer cells. ShyMs, similar to Boyden chambers, are compatible with standard well-plates designs and can be printed using commonly available 3D printers. In the future, ShyM can be potentially extended to variety of photosensitive hydrogels and cell types, to develop new in vitro assays to investigate complex cell–cell and cell–extracellular matrix (ECM) interactions. [DOI: 10.1115/1.4031467]

Manuscript received June 29, 2015; final manuscript received August 25, 2015;
published online September 29, 2015. Assoc. Editor: Ibrahim Ozbolat.

1 Introduction

For the past several decades, the need of recreating an in vivo like environment has driven researchers to develop new and improved cell culture platforms for basic and applied life sciences. Traditional 2D cultures do not recapitulate the complex cell-cell and cell-ECM interactions [1]. In 2D cultures, cells polarize in an attempt to increase their exchange area to culture media, resulting in excessive nutrition and oxygenation and an absence of biochemical gradients [2,3]. Permeable supports or membrane filters such as Boyden chamber (transwells), with dual media exposure, allow cultured cells to carry out metabolic functions in an in vivo-like manner. A Boyden chamber also allows an easy-to-use well-plate configuration and therefore has been widely accepted in variety of applications including cellular invasion, permeability, drug-transport, co-culture, and tissue remodeling to name a few [4–6]. However, the membrane used in Boyden chamber is typically stiff with low porosity (max 10%) and does not recapitulate the material (stiffness) or structural (porosity) of in vivo 3D ECM.

To capture the complexities of the native ECM in a 3D in vitro model, various approaches have been developed. One such approach has been the use of multicellular spheroids, which produce hollow cores and partially reestablish 3D environment; however, spheroids grow as independent cellular aggregates and minimally interact with the surrounding ECM [7]. Advances in biomaterials and microfabrication have resulted in new physiologically relevant in vitro assays using biomaterials derived from ECM of both natural and synthetic origins [8]. For example, gel-embedding assay involves seeding cells on top of a thin or thick (few millimeters) layer of fluorescently labeled Matrigel or collagen to monitor 3D vertical invasion of cells into ECM [9,10]. Synthetic hydrogels such as polyethylene glycol (PEG) functionalized with cell-signaling motifs have also been used as artificial ECM with tunable physical and biochemical properties [1,7,8,11]. Newer approaches such as "tissue-on-a-chip" utilize assembly of robust components such as the stiff membranes (similar to the one used in Boyden's chambers) to develop novel biosystems [12]; however, important challenges such as low scalability of the fabrication methods remains unresolved.

Few researchers have combined the Boyden chamber approach with collagen by eliminating the nonphysiological stiff membrane and suspending collagen membrane between side supports, thus creating a biomimetic culture platform [13,14,15,16]. For example, a casting method was used to create a thin layer of collagen between supports to mimic the glomerulas interface in kidneys with juxtaposition of podocytes and endothelial cells on either sides of the collagen film [15]. Another group employed a similar floating thin fibrillar collagen gel layer supported by rigid nylon support to investigate how physical boundaries interrupt the cell–collagen interactions based on the strain-stiffening nature of collagen [16]. Restrained and floating collagen matrix with seeded fibroblasts were also used to investigate matrix remodeling before or after developing isometric tension and associated changes in stress fibers [14]. In this work, we chose to use GelMA, a photo-crosslinkable hydrogel extensively used in the field due to several favorable properties such as presence of cell-binding (and degradation) sites and relatively ease of control over its physical stiffness [17–20]. In this work, we developed a permeable suspended GelMA hydrogel membrane or ShyM that has dual media exposure and is compatible with standard well plate configurations. As compared to the previous studies, the ShyM platform developed in this work has tunable thickness and mechanical properties and can be printed using a commercially available 3D printer. Most importantly, ShyM has the ability to encapsulate living cells within the gelatin membrane, a research direction not explored by earlier studies. Last, the Boyden-chamberlike design is easy to use due to its compatibility with well plates and established imaging and analysis protocols. We believe that, similar to Boyden's chamber, ShyM could potentially find applications in a wide variety of high-throughput cellular assays.

2 Materials and Methods

2.1 GelMA Synthesis. GelMA was synthesized using an established protocol [17–20] (Fig. 1(*a*)). Briefly, porcine skin gelatin (Sigma Aldrich, St. Aldrich, St. Louis, MO) was mixed at 10% (wt./vol.) in phosphate buffered saline (PBS; Gibco, Billings, MT) and stirred at 45 °C until fully dissolved. Methacrylic anhydride (Sigma) was added to the solution at the rate of ~0.5 ml/min to get a concentration of 8% (vol/vol) of MA in gelatin solution. This mixture was stirred for 3 hrs before dialyzing against distilled water (12–14 kDa cutoff dialysis tubing (Spectrum Laboratories, Inc., Rancho Dominguez, CA) for 1 week (40 °C) to remove the unreacted groups from the solution. The dialyzed GelMA solution was lyophilized in a freeze dryer (Labconco, Kansas City, MO) for one week. Addition of methacrylamide moieties to the side group of natural gelatin enables the UV-crosslinking approach. Three GelMA prepolymer solutions were prepared by mixing the freeze dried GelMA with PBS at 40 °C at various amounts (7%, 10%, and 15% wt./vol.). Each prepolymer solution was mixed with UV (ultraviolet) photoinitiator Irgacure 2959 (0.1%, Specialty Chemicals, Basel, Switzerland). The degree of methacrylation (DOM) was calculated as the percentage of modified lysine groups and quantified using ^{1}H NMR [18,21]. ^{1}H NMR spectra of GelMA recorded in D_2O at room temperature [Supplemental Fig. S2(*c*) is available under the "Supplemental Data" tab for this paper on the ASME Digital Collection]. The peaks H^a and H^b showed the incorporation of double bonds into the gelatin where A showed aromatic residues from the unmodified gelatin. The DOM was determined by comparing the integrated intensity of double bond region to the intensity of the aromatic region.

2.2 ShyM Fabrication. An open-grid structure [Figs. 1(*b*) and 1(*c*); Supplemental Fig. S1(*a*) is available under the "Supplemental Data" tab for this paper on the ASME Digital Collection] was printed in polylactic acid (PLA) polymer using a commercial printer (Makerbot) with optimized printing parameters (100% infill; layer thickness = 0.1 mm; extruder temperature = 230 °C, extrusion speed = 75 mm/s). Grid-insert (min resolution, ~300 μm) was placed in a 24-well plate, and GelMA prepolymer solution (150 μl of GelMA prepolymer solution) was added to the grid, and subsequently exposed to UV light (Omnicure S2000 Lamp, 365 nm wavelength) for 100 s, which resulted in crosslinking of a stable suspended membrane (~250–1000 μm) to the PLA grid. For prototype 1, ShyMs were formed on the PLA grid and then assembled between the top and bottom inserts (Fig. 1(*b*)), while for Prototype 2, ShyMs were formed after placing them in a 24-well plate (Fig. 1(*c*)), without the need of ShyM assembly postprocessing steps. ShyMs were subsequently incubated in PBS at 37 °C for future cell culture experiment. For cell encapsulation experiments, 15% GelMA solution was mixed with cell suspension of 1-to-1 ratio to achieve a final concentration of 7.5% (wt./vol.) GelMA and followed by ShyM fabrication. Prepolymer solution with less than 5% GelMA resulted in unstable films and cannot be used for fabricating ShyMs [Supplemental Fig. S1(*g*) is available under the "Supplemental Data" tab on the ASME Digital Collection].

2.3 Characterization of ShyMs

2.3.1 Thickness. ShyM thickness was controlled by changing the size of the supporting PLA grid [Supplemental Fig. S1(*b*) is available under the "Supplemental Data" tab for the ASME Digital Collection]. Thickness was determined by taking cross-sectional images using a 3D digital microscope (Hirox, Pennsylvania). ShyMs were incubated in PBS at 37 °C for 1–3 days, transversely cut and imaged [Supplemental Fig. S1(*c*) is available

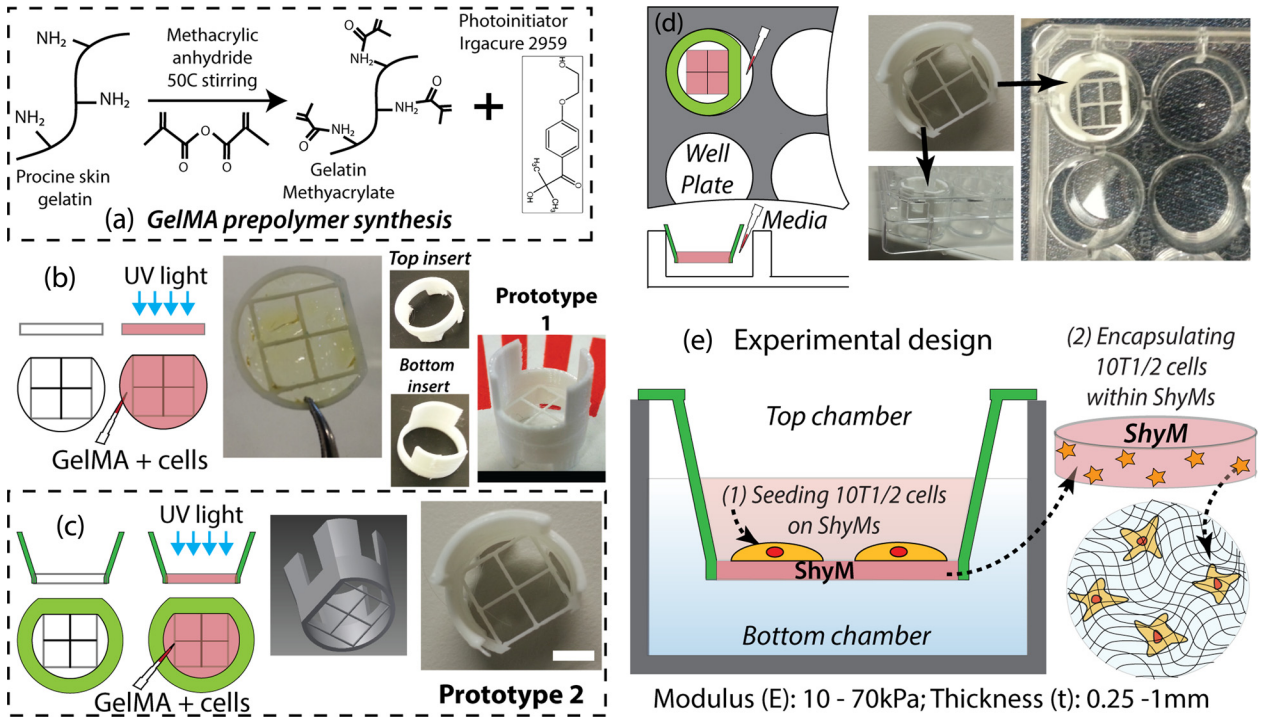

Fig. 1 Design and fabrication of suspended hydrogel membrane (ShyM): (*a*) Process flow to synthesize photosensitive gelatin methacrylate (GelMA) prepolymer solution. Two prototypes were developed in polylactic acid (PLA) using a 3D printer. Ultraviolet light (UV) was used to crosslink photosensitive GelMA solution to form a membrane suspended between the PLA grids. Prototype 1 (*b*) consist of three separate parts: the top and bottom inserts and membrane insert. The membrane insert with a yellow food dye is depicted in the photograph. Prototype 2 (*c*) is a monolithic construct printed using a 3D printer. GelMA with or without cells can be suspended to form a membrane with dual fluid exposure. Scale bar: 5 mm. (*d*) Prototype is designed to fit within a standard 24 well plate. The side gap facilitates ease of changing media during cell culture experiments. (*e*) Two cell-culture conditions were tested using C3H/10T1/2 murine mesenchymal progenitor cells. Cells were either seeded on top of ShyMs (1) or encapsulated within ShyMs (2). ShyM modulus was varied from 10 kPa to 70 kPa by varying the concentration of GelMA, while its thickness was modulated by controlling the size of the PLA support grids.

under the "Supplemental Data" tab for this paper on the ASME Digital Collection]. For testing bulk properties of GelMA ShyMs including mass swelling, storage and compressive modulus, and diffusion constants, disk shaped samples were prepared (5 mm diameter; 1.6 mm thickness) using a Teflon mold and the UV exposure conditions similar to one used for fabrication of ShyMs.

2.3.2 Mass Swelling Ratio. GelMA samples (7%, 10%, 15%) were incubated in PBS at 37 °C for 24 hrs and dried overnight at room temperature. The swelling ratio was measured by comparing the swollen weight over the dried weight, as follows: Swelling ratio (%) = [(Ww–Wi)/Wi] × 100% (Ww: wet weight of hydrogel; Wi: initial (dry) weight of hydrogel sample). The swelling reaches a stable state after 1 day incubation in PBS and facilitates repeatable measurements.

2.3.3 Cross-Sectional Swelling. Swelling of GelMA–ShyMs within the PLA grid was characterized using a digital optical microscopy (Hirox, Pennsylvania). GelMA–SHMs were incubated in PBS at 37 °C for 2, 48 and 168 hrs, and PLA grid was cut transversely to obtain unrestrained state of one side of GelMA-SHMs [Supplemental Figs. S1(*c*) and S1(*h*) are available under the "Supplemental Data" tab for the ASME Digital Collection]. The dimensions of the unrestraint side, which was free to swell as it absorbs PBS, was quantified after 2 hrs and 2 and 7 days.

2.3.4 Compressive Modulus. Compressive modulus was characterized using a Q800 Dynamic Mechanical Analysis (DMA) (TA Instruments, Inc.). Disk GelMA samples (7%, 10%, 15%) were incubated in PBS at 37 °C for 48 hrs, and loaded under compression and tested for controlled strain percentage (ramping from 0% to 40%) with preloaded force of 0.01 N with displacement of 10 μm. The slope of stress–strain curve from 0% to 10% strain was used to determine compressive modulus [Supplemental Fig. S2(*b*) is available under the "Supplemental Data" tab on the ASME Digital Collection].

2.3.5 Viscoelastic Properties. Rheological time-sweep was used to monitor the changes in the storage modulus as a function of UV-light exposure time. We modified a standard AR 2000 Rheometer (TA Instruments) with a 45 deg reflective mirror and a custom-made insert for enabling attachment of UV-light collimating tube from a S2000 UV lamp (Omnicure) [Supplemental Fig. S2(*a*) is available under the "Supplemental Data" tab on the ASME Digital Collection]. UV was in on and off states for 100 s. This time was chosen to simulate the approximate time of UV exposure used for ShyMs. The frequency used was 1 Hz, and straining shear stress was 1 Pa during the test. With UV exposure of 100 s, we see an increase in the G' property of the prepolymer hydrogel indicating the hydrogel crosslinking process as a function of time.

2.3.6 Diffusion Properties. To analyze the diffusive properties of GelMA with varying concentrations (7%, 10%, and 15%), fluorescent proteins of 70 kDa (Sigma Aldrich, St. Aldrich, St. Louis, MO) were quantified. A relationship between the pore-parameters and diffusion parameter was obtained using established protocols [22,23]. Samples were incubated for 48 hrs to achieve a quasi-steady-state and subsequently incubated in 3 mg mL^{-1} FITC-Dextran/PBS solution of fluorescent molecules to allow dye-diffusion. The structure will then be irradiated with blue light ($\lambda = 488$ nm) to make a 50 μm-diameter spot with an incident power of 25 mW to create a darkened photobleached

region. A MATLAB algorithm was used to determine the radius of the bleached area as the average distance at which the fluorescent intensity falls a certain preset value of the maximum value taken from the center of the bleached image. The mean fluorescent intensity was calculated for each image over the recovery period and converted to diffusion coefficients using a previously described method [22,23]. Briefly, a 2D xy planar configuration is assumed, and diffusion in and out of the 2D plane (z direction) is neglected. The diffusion of fluorescent tracer molecules within this darkened region was tracked and quantified by image analysis to empirically determine the diffusion parameter for each sample. The normalized fractional fluorescence intensity f was calculated as using the following equation: $f = [F(t) - F(0)]/[F(\infty) - F(0)]$, where $F(t)$, $F(0)$, and $F(\infty)$ are fluorescence intensity at time (t), immediately after bleaching, and after complete recovery respectively. The fractional intensity f was plotted versus time and fitted with a logarithmic curve, and $f(t = 0.5)$ or half-recovery time τ was determined. Diffusion parameter D was determined by the following equation, $D = [\omega^2/4\tau](\gamma_D)$, where ω = measured spot radius; γ_D is the bleaching parameter. The diffusion data for 7%, 10%, and 15% GelMA concentration was quantified.

2.3.7 SEMs. GelMA samples (7%, 10%, and 15%) were freeze-dried, sputter coated for 45 s, mounted on an aluminum SEM stubs with double-sided carbon tape, and imaged using Scanning Electron Microscopy (Joel 5600, Japan) at 10 kV [Supplemental Figs. S2(d)–S2(f) are available under the "Supplemental Data" tab on the ASME Digital Collection].

2.4 Cell Culture and Immunohistochemical Staining. C3H/10T1/2 murine mesenchymal progenitor cells (10T1/2 s) were cultured in BME supplemented with 10% fetal bovine serum, 1% Glutamax, and 1% Penstrap and were maintained in a 37 °C incubator with 5% CO_2. Cells were passaged using standard cell culture protocols using 0.25% Trypsin/EDTA and were used within passage number 15. Cells were harvested, counted, and either seeded on or encapsulated within GelMA–ShyMs. Media was changed every other day. Cells were fixed at various time points using 4% paraformaldehyde (Invitrogen, Carlsbad, CA) overnight at room temperature and permeabilized with 0.1% Triton X-100 (Sigma Aldrich) in PBS with 1% bovine serum album (Sigma Aldrich) for 30 mins. For F-actin and nuclei staining cells were labeling secondary antibodies (Alexa 488 or Alexa 647, Invitrogen, Carlsbad, CA) and Hoechst 33l258 DNA dye (Invitrogen, Carlsbad, CA) for 30 mins. Confocal fluorescence imaging was performed using Zeiss LSM 710, and image analysis was performed using ImageJ. Cell proliferation assay was performed using a Cell Counting Kit-8 (Dojindo) according to the manufacturer's instructions. 10T1/2 s were seeded onto the ShyM and let it attached before adding CCK8 solution. The number of viable cells at various time points were measured by reading absorbance at 450 nm using a microplate reader (FLx800, Bio-Tek Instruments). Cell culture medium was changed every other day on both top and bottom chambers. Cell concentration is 4×10^5 cells/ml.

The Click-iT EdU proliferation assay was used to characterize the mitotic rates of encapsulated cells within the ShyMs and flat controls. EdU (5-ehynyl-2′-deoxyuridine) was added to media 5 days postencapsulation. Following fixation after 48 hrs, Alexa 555 (red) was used to label the EdU via Click chemistry to visualize the proliferative cells. Quantification of proliferation was done on ImageJ via "3D Objects Counter" plug-in using z-stack pictures. Seeded cells and encapsulated cells were stained using calcein-AM/ethidium homodimer (Invitrogen, Carlsbad, CA) at various time points and visualized using 488 and 543 nm lasers to characterize cell viability. Quantification of dead cells (red) and live cells (green) was done on ImageJ by setting the proper threshold. Images were incorporated into ImageJ to compare the long axis and short axis of nuclei using the "Shape Descriptors" plug-in.

2.5 Statistical Analysis. All quantitative values are reported as means ± standard deviation with at least $n = 3$ samples per group. One way analysis of variance was performs using SigmaPlot 12.5 (Systat Software Inc., San Jose, CA). P values <0.05 were considered statistically significant, P values <0.01 and <0.001 were considered highly statistically significant.

2.6 Cell Invasion Using ShyM. MDA-MB-231 cells were cultured in high glucose DMEM containing 10% fetal bovine serum (FBS) and antibiotic/antimycotic (ABM). Following 2 hrs sterilization of ShyMs using UV light, 10 000 cells/well were plated in 250 μl of FBS-free DMEM with ABM. Cells were allowed to invade toward media containing 10% FBS for 24 hrs. Calcein AM was diluted 1:1000 in serum free medium and added to cells for 30 mins at 37 °C. Fresh serum free media was added to replace the staining solution, and cells were imaged using a Nikon Eclipse

TE2000-E multimode epifluorescence microscope equipped with 10× Plan Fluor objective and a Hamamatsu ORCAII CCD camera and driven by the Nikon Elements software.

3 Results and Discussion

In this work, we design a ShyM biosystem by combining the advances in biomaterial science and 3D printing technology. GelMA ShyMs provides fluid exposure from the top and bottom sides, allows modulation of its physical and cellular properties, and facilitates incorporation of living cells using cell-seeding and cell-encapsulation approaches.

3.1 GelMA Synthesis and ShyM Fabrication. Gelatin is denatured collagen and has integrin cell-binding motifs, such as Arg-Gly-Asp (RGD), and matrix metalloproteinases (MMP) degradable sites. Another important advantage of GelMA is that the physical stiffness can be tuned by altering the polymer dry mass (% prepolymer). We synthesized GelMA hydrogel with varying concentrations (7–15%) using an established protocol [17–20] (Fig. 1(a)). Methacrylamide moieties added to the side group of natural gelatin enables crosslinking by UV light. ^{1}H NMR was used to determine the DOM to be 70% [Supplemental Fig. S2(c) is available under the "Supplemental Data" tab on the ASME Digital Collection].

A critical component to the design was to create a suspended structure between the PLA struts that would facilitate fluid exposure from two sides. Surface tension allows the formation of GelMA ShyMs between PLA grid structures as described in Sec. 2. In this process, a photo-initiator in the GelMA prepolymer solution initiates the crosslinking reaction upon exposure to UV light. UV light generates free radicals, and, in their presence, activates functional monomers to form covalent bonds and develops a 3D crosslinked hydrogel membrane suspended between PLA grid structures. Below 5% GelMA concentration, the membrane does not have enough surface tension to form a stable suspended membrane [Supplemental Fig. S1(g) is available under the "Supplemental Data" tab on the ASME Digital Collection]. However, a decrease in the grid-spacing could achieve a stable ShyM with lower GelMA concentrations (data not shown). The thickness of ShyMs can be easily controlled by changing the size of the supporting PLA grid from 240 to 960 μm (Fig. 2(a)). Thickness was determined by taking cross-sectional images of the PLA grid and the ShyMs. Even after the cut [Supplemental Fig. S1(h) is available under the "Supplemental Data" tab on the ASME Digital Collection], the ShyMs were robust and maintain their structure for more than 4 weeks. For both cell-seeding and cell-encapsulation experiments, we have used the prototype 2 (Fig. 1(c)–1(e)), a monolithic insert that fits within a standard 24-well plate. However, an open grid insert can also be developed [Fig. 1(b); Supplemental Figs. S1(a)–S1(f) are available under the "Supplemental Data" tab on the ASME Digital Collection], which

has to be assembled within the top and bottom inserts. Prototype 2 is a one-piece insert that required no assembly, while prototype 1 requires assembly but has more experimental flexibility. Both prototypes allow for the suspended design and do not require any rigid support such as silanized glass or stiff polymer inserts commonly used in Boyden's chambers.

3.2 Determination of Physical Properties. ShyM properties such as swelling ratio, compressive and storage modulus were quantified as a function of % GelMA prepolymer (7, 10, and 15). Swelling ratio was quantified using two approaches. First approach used standard disk samples, while the second approach transversely cut the ShyMs and quantified the change in thickness as a function time. Mass swelling ratio decreases with an increase in GelMA concentration: 7% (0.93) and 10% (0.91) GelMA was significantly higher than 15% GelMA (0.83) (Fig. 2(*b*)). Swelling of ShyMs were also quantified by cutting the PLA grid and measuring the changes in thickness as a function of incubation time in PBS (Fig. 2(*c*)). The unrestraint side of the transversely cut ShyMs [Supplemental Fig. S1(*c*) is available under the "Supplemental Data" tab on the ASME Digital Collection] freely swells to absorb PBS. We observe a steady increase in the swelling thickness of ShyM with time for both 7% and 10% GelMA; however, a minimal change with 15% GelMA possibly due to smaller pore sizes with 15% GelMA. Moreover, 7% GelMA swells significantly more as compared to the 10% and 15% GelMA. Few ShyM samples were incubated in PBS for 4 weeks, and thickness was evaluated by transverse cutting of the ShyM membrane [Supplemental Fig. S1(*h*) is available under the "Supplemental Data" tab on the ASME Digital Collection]. We found that the thickness did not significantly change and was similar to ShyM samples that were incubated in PBS for only 2 hrs, suggesting that PLA grids constraint the swelling of ShyMs, a probable reason for its long-term stability and robustness [Fig. 2(*d*); Figs. S1(*c*) and S1(*h*) are available under the "Supplemental Data" tab on the ASME Digital Collection].

Viscoelastic properties of GelMA were characterized using a custom-built rheometer setup [Fig. S2(*a*) is available under the "Supplemental Data" tab on the ASME Digital Collection]. With UV exposure, we observe an increase in storage modulus (G') indicating the dynamics of the crosslinking process as a function of time. The exposure time of 100 s was chosen to simulate the UV exposure used for fabrication of ShyMs. Compressive modulus as characterized by DMA reveal a positive correlation between GelMA concentration and stiffness for three batches tested (Fig. 2(*f*)).

Because diffusion properties of hydrogels play an important part in cell viability and function [24,25], we quantified the diffusion properties of 7%, 10%, and 15% GelMA samples by fluorescence recovery after photobleaching (FRAP) method [22,23]. A 70 kDa FITC-dextran similar in size to serum albumin protein was used. For both 7% and 10% GelMA, the recovery fraction was close to 1, while for 15% GelMA there was a decrease in recovery, indicating that majority of FITC-dextran was mobile with the 7% and 10% GelMA, while 15% GelMA concentration was marginally linked to diffusive properties [Fig. 2(*g*); Supplemental Fig. S2(*g*) is available under the "Supplemental Data" tab on the ASME Digital Collection]. SEM images showing pores in all GelMA samples with pore size ranges from 10 to 400 μm^2, where 15% GelMA was found to have compact aligned pores as compared to 7% and 10% GelMA, although these results are not significantly different [Supplemental Figs. S2(*d*)–S2(*f*) are available under the "Supplemental Data" tab on the ASME Digital Collection].

3.3 Cell Seeding on ShyMs. GelMA is transparent and readily permits microscopic analysis of cells seeded on or embedded within ShyMs. C3H/10T1/2 murine mesenchymal progenitor cells (10T1/2 s) were seeded on top of 7%, 10%, and 15% ShyMs, and were stained using a calcein-AM/ethidium homodimer, and labeled for f-actin (green) and nuclei (blue) (see online version for color). An increase in the overall intensity as well as distribution of actin staining (intensity increases as we toward the periphery of cells and away from the nuclei) as we increase GelMA concentration (Figs. 3(*a*) and 3(*b*)); however, this was an observed trend but we were not able to quantify because of several overlapping cells. As a result, we quantified the changes in the nuclear aspect ratio as an indicator of the overall aspect ratio of the seeded cells. An increase in the GelMA concentration resulted in an increase in the nuclear aspect ratio (Fig. 3(*e*)), probably because of either changes in modulus and associated changes in cell-ECM interactions; however more experiments have to be performed to elucidate the exact mechanism. The "flat" control is 10% GelMA casted onto a modified glass with media exposure from only one side [Fig. 3(*c*); Supplemental Figs. S3(*e*) and S3(*f*) is available under the "Supplemental Data" tab on the ASME Digital Collection]. We observe no change in the viability of cells on ShyMs as compared to the "flat" controls (Fig. 3(*d*)). After 2 hrs postseeding, cell proliferation of 7%,10%, and 15% ShyMs was higher than the flat control, as well as tissue culture polystyrene (TCPS) control, exhibiting high seeding efficiency and cell adhesion (Fig. 3(*f*)). The proliferation on all ShyMs (7%, 10%, 15%) continue to be significantly higher compared to flat controls for at least 48 hrs. ShyMs are compatible with standard cell culture protocols and were handled similar to cells grown on glass coverslips or TCPS well plates.

3.4 Cell-Encapsulation Within ShyMs. All cell encapsulation experiments were conducted using 15% GelMA solution. Figures 4(*a*)–4(*d*) demonstrate the spreading of encapsulated 10T1/2 cells and its actin distribution as a function of time. Cells encapsulated within ShyMs rapidly spread and reach a network like structure by day 7 as compared to the relatively round cell morphology on the flat control sample on day 7. Nuclear aspect ratio of encapsulated cells within ShyMs on day 4 and day 7 are significantly higher as compared to encapulated cells for day 2 as well as flat controls on day 7 (Fig. 4(*f*)), probably a function of dual-media exposure, although detailed experiments have to be performed to investigate mechanism. Viability of encapsulated cells at day 2 did not show any differences between ShyM and flat control samples (Figs. 4(*g*) and 4(*h*)). The oblong shape of the cells is a result of an artifact of confocal imaging. However, viability of encapsulated cells at day 7 showed a big difference between the ShyMs and flat control samples as higher viability showed in ShyMs [Supplemental Figs. S3(*c*) and S3(*d*) are available under the "Supplemental Data" tab on the ASME Digital Collection], possibly due to one-sided media exposure for the flat controls. Encapsulated cells within ShyMs exhibited greater proliferative activity (day 5) overall compared to flat controls (Figs. 4(*I*) and 4(*J*)). ShyMs with encapsulated cells were found to be stable more than 4 weeks for 7% GelMA and more than 6 weeks for 15% GelMA.

3.5 Case Study: Cell Invasion Using ShyMs. Cell migration and invasion through the extracellular matrix plays an important role in normal physiological processes such as morphogenesis and immune surveillance, as well as in disease processes. One example of the pathologically enhanced migration and invasion is the process of cancer metastasis in which tumor cells breach the basement membrane surrounding the tumor, invade adjacent tissues, and spread to new sites via the circulation [26]. ShyMs represent a potential avenue for creating flexible substrates similar in thickness, composition, and mechanical properties to the tumor stroma. As an example of how tumor cell invasion assay can be set up using ShyMs, we performed an experiment in which highly invasive breast cancer cells (MDA-MB-231 cell line [27]) were added to the top surface of ShyM inserts, and cell invasion was observed over time using

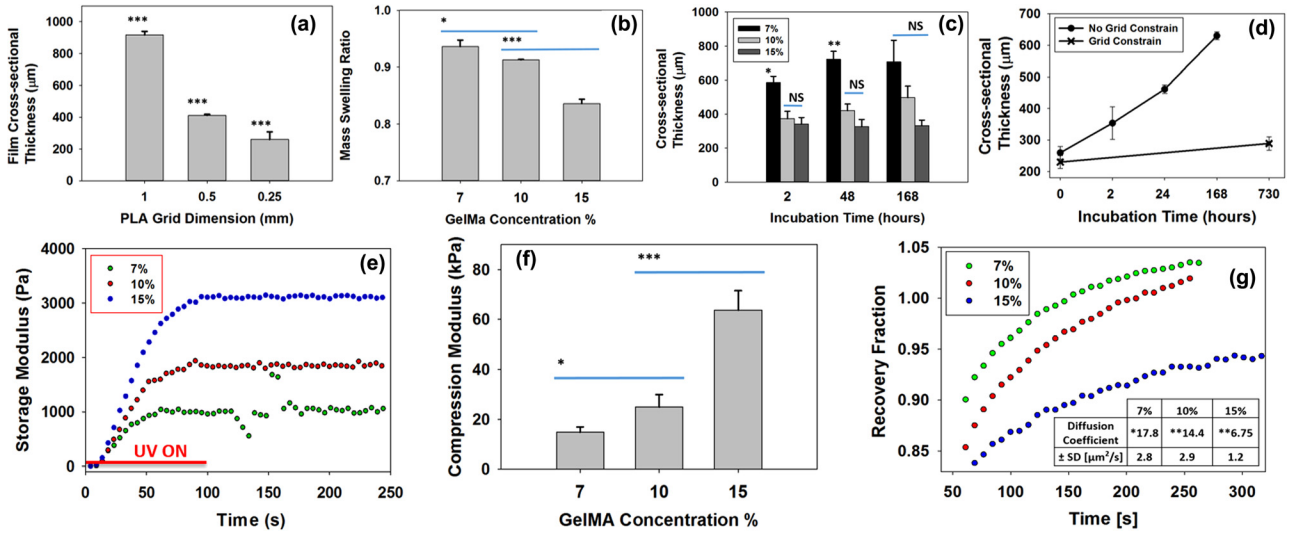

Fig. 2 Characterization of ShyM properties: (*a*) The thickness of ShyMs can be varied by controlling the PLA grid size. As compared to the PLA grid, ShyM thickness is smaller, however, highly repeatable. (*b*) Mass swelling measurements demonstrate that 15% GelMA is significantly lower as compared to 7% and 10% GelMA. (*c*) GelMA ShyMs formed within PLA grids were transversely cut to expose the side section of the membrane, and incubated in PBS for 2 hrs and 2 and 7 days. We observe significant differences between swelling properties of 7% ShyMs till 0–2 days as compared to 10% and 15% GelMA ShyMs. (*d*) ShyM swelling with and without the PLA-grid demonstrate the contribution of PLA grid in constraining the transverse swelling response of ShyMs. (*e*) A custom-made rheometer setup was developed to measure the change in storage modulus as a function of UV exposure time. A time of 100 s was chosen to simulate UV exposure time for crosslinking the ShyMs. A higher storage modulus is observed for 15% GelMA as compared to 7% and 10% GelMA. (*f*) Dynamic mechanical analyzer (DMA) was used to measure the compressive modulus, and the slope between 0% and 10% was considered for analysis. Results demonstrate that both 15% and 10% GelMA have significantly higher modulus as compared to 7% GelMA. (*g*) Diffusion constants of 7%, 10%, and 15% GelMA were calculated by using 70 kDa FITC-dextran for FRAP analysis. Results show the diffusion coefficient of 15% are significantly lower than 7% and 10%. Data plotted as mean and standard deviations: *, $P<0.05$; **, $P<0.01$; ***, $P<0.001$.

vital cell staining with Calcein AM. As shown in Fig. 5, the cells have rapidly spread on the top surface of the insert and over the course of 24 hrs some of the cells have invaded through the insert towards the bottom surface. This experiment demonstrates the utility of ShyMs for studies of cancer cell migration and invasion.

Advanced in microfabrication and biomaterials have results in the development of new and improved biosystems capable of elucidating new cell–cell and cell–ECM relationships. Hydrogels have emerged as the ideal matrix to investigate cell–materials interaction in 3D environments. Crosslinked hydrogels are prepared using variety of approaches such as ionic interactions, *p*H

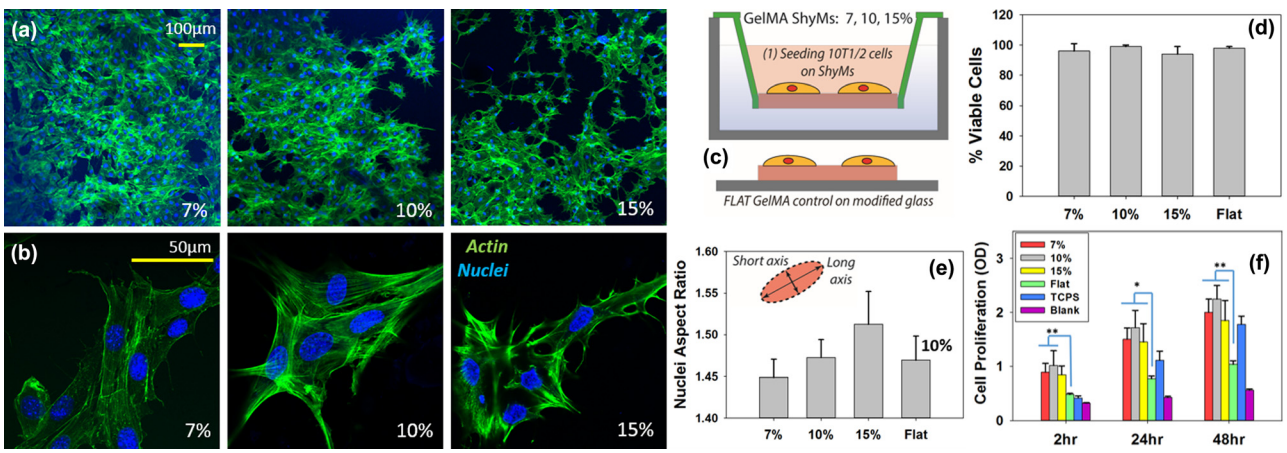

Fig. 3 Murine mesenchymal 10T1/2 cells were seeded on 7%, 10%, and 15% ShyMs and control flat samples adhered to a modified glass substrate, and viability, proliferation and nuclei aspect ratio were characterized: (*a* and *b*) representative images of cells seeded on 7%, 10%, and 15% GelMA ShyMs at 10× and 63× magnifications. Cells were stained for F-actin (green) and nuclei (blue). (*c*) Schematic depicts the experimental design of ShyMs as well as flat control sample. (*d*) Viability of 10T1/2 cells seeded on GelMA ShyMs was assessed via calcein-AM/ethidium homodimer LIVE/DEAD assay at 48 hrs post-seeding. Results demonstrate no change in viability of cells when compared to flat control. (*e*) Aspect ratio was calculated by comparing the ratio of the long axis of nucleus with the short axis. Although not statistically significant, we observe a trend of increasing aspect ratio with increased GelMA concentration. Control used in this case is using 10% GelMA. (*f*) Proliferation was conducted using CCK-8 assay, and the absorbance value was compared with flat control (10% GelMA) as well as TCPS and blank (cck-8 and media only). The proliferation of cells seeded on all ShyMs are higher that of all flat controls at three time points. Error bars represent the SD of at least three independent samples: *, $P<0.05$; **, $P<0.01$; ***, $P<0.001$.

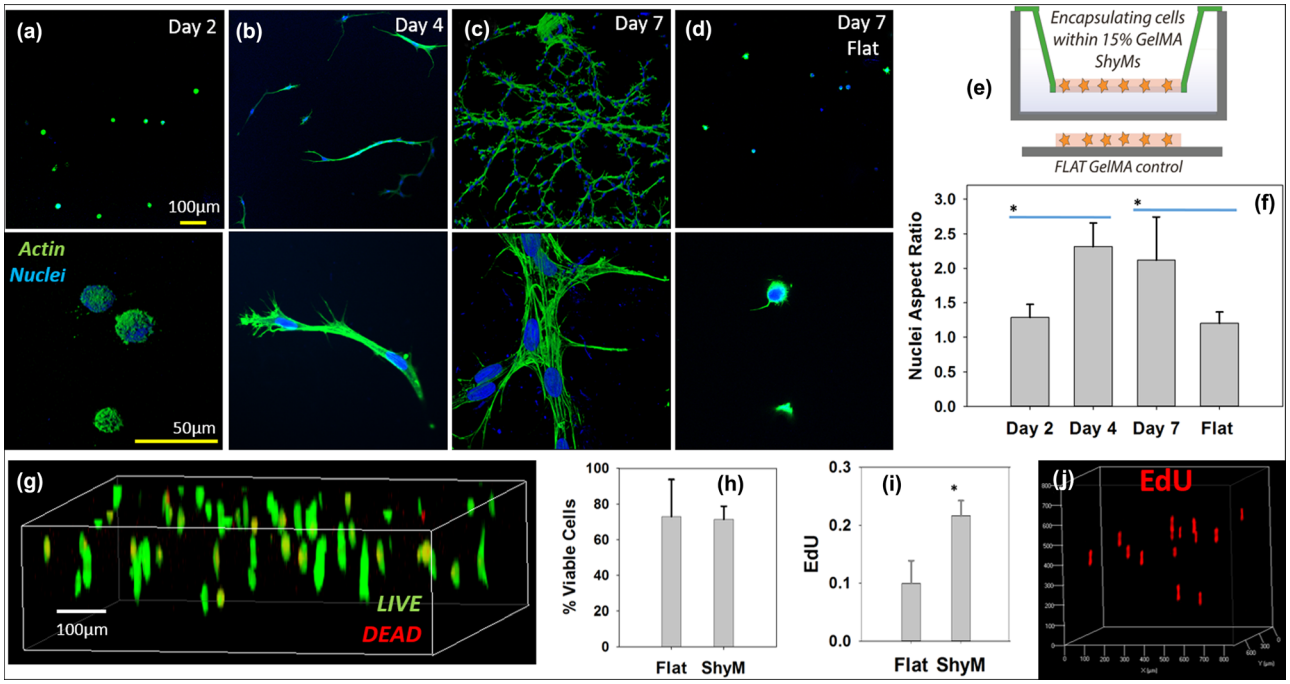

Fig. 4 Cell encapsulation of 10T1/2 cells within 15% GelMA ShyMs: (*a* to *d*) ShyMs with encapsulated cells were stained for F-actin and nuclei and fluorescence micrographs were captured at 10× and 63×. Cells appear round in shape on day 2 post-encapsulation but spread at day 4 and form an interconnected network on day 7 as compared to flat control. (*e*) Schematic of experimental design. (*f*) Aspect ratio of nuclei were calculate. Results show statistical significance between aspect ratio at days 4 and 7 as compared to both day 2 within ShyMs as well as flat control samples. (*g* and *h*) Viability of 10T1/2 cells encapsulated in ShyMs was assessed via calcein-AM /ethidium homodimer at 48 hrs post-encapsulation. High cell viability was maintained in ShyMs. (*i* and *j*) The Click-iT EdU assay was performed at day 5 to assess the proliferative ability of 10T1/2 cells throughout the ShyM (labeled with Alexa 555). Results demonstrate higher proliferation within ShyM as compared to controls. Error bars represent the SD of at least three independent samples: *, $P < 0.05$; **, $P < 0.01$; ***, $P < 0.001$.

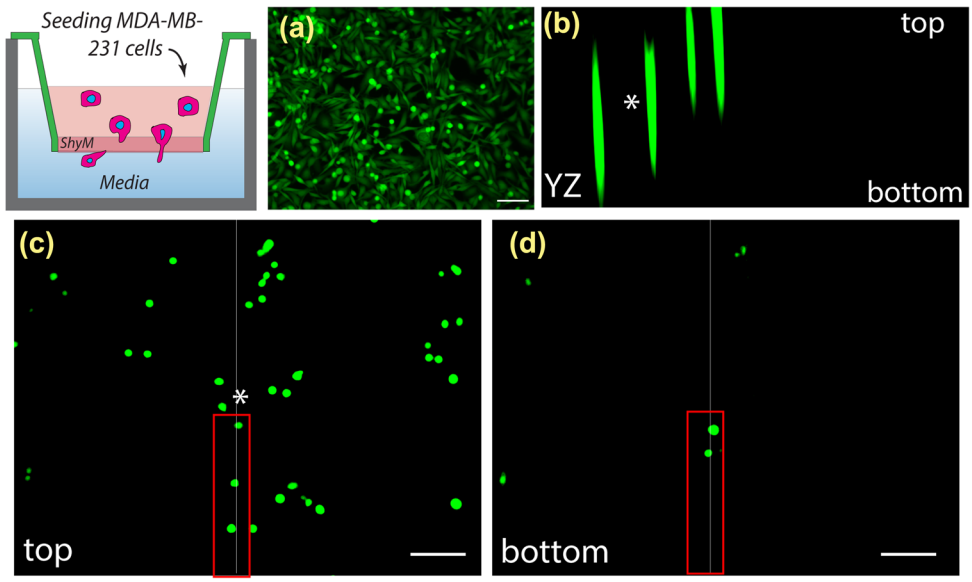

Fig. 5 (*a*) MDA-MB-231 cells plated densely on 10% GelMA ShyMs and stained with Calcein AM. These cells are located on top surface of the ShyM. (*b*) Side view (YZ projection) of MDA-MB-231 cells migrating into the ShyMs 1 day post-plating. It is clear that some cells are no longer at the top but are invading downward (*). (*c* and *d*) Top and bottom optical sections for the same field of view as the one shown in (*b*) and (*c*) shows cells near the top of the ShyMs that have not invaded, while (*d*) represents cells that have invaded. The line in these images represent the cross section taken to create the orthogonal projections shown in (*b*). Scale bars, 100 μm.

stimulation, and photocrosslinking using UV) [28–30]; however, solution casting along with UV light is the method of choice because its precise control over the crosslinking process as well as its ease of use. Typically, hydrogel prepolymer solution is cast into molds to develop flat disk shaped crosslinked hydrogels. Typically in this case, the crosslinked hydrogels are only exposed to media from only one side, while the other side is stuck to a substrate. In this work, we report the design and development of a novel ShyM with Boyden-chamber like supports (printed using a commercially available 3D printer), and demonstrate the broad applicability with cell seeding and cell encapsulated approaches.

We chose GelMA (type 1 collagen) to develop ShyMs as it is commonly used in coating tissue culture plate to promote cell growth. GelMA also possesses cell-binding and cleavage sites, while its chemical modification (by introducing methacrylamide side groups) allows the control of its mechanical properties (via chemical crosslinking reaction). The ability to control the physical and biochemical of hydrogel matrix could potentially influence variety of cellular processes such as proliferation, differentiation in physiological and pathological conditions [31–35]. A significant advantage of ShyMs is the absence of any underlying rigid substrate (support), typically used in hydrogel culture. GelMA ShyMs developed in this work has the advantage of high transparency and permitting microscopic analysis of cells embedded within these matrices. ShyMs with controlled thickness would function as a free-standing biomimetic membrane planar support to culture cells, potentially allowing close juxtaposition of living cells on either side of the membrane, developed using variety of photosensitive biopolymers [36–38]. ShyMs compatibility with standard imagining techniques opens doors to variety of applications in co-culture studies, tissue modeling studies, cell signaling, cell invasion and migration [14].

4 Conclusions

In this work, we develop a ShyM platform using GelMA hydrogel, by combining 3D printing technology with biomaterial science, to demonstrate the broad applicability with cell culture approaches. The free-standing nature of ShyM not only allows dual media exposure but also provides control over its physical properties and cell incorporation methods (seeding and encapsulation). ShyMs are compatible with standard well-plates designs and can be printed using commonly available 3D printers. ShyM can be potentially extended to variety of photosensitive hydrogels and cell types, to develop new in vitro assays to investigate complex cell-cell and cell-ECM interactions.

Acknowledgment

We acknowledge Syracuse Biomaterial Institute for providing equipment used for all the experiments in this paper. We thank Can Aslan for his contribution on the preliminary design and Makerbot troubleshooting, Ciba Specialty Chemicals for photoinitiator samples, the Biology department of Syracuse University for usage of Confocal facility, Dr. Henderson's group for their generous donation of 10T1/2 cells, Richard Baker for the cell-culture protocols, and Yangping Liu for SEM training. P.S. conceived the project. Y.X.C, and P.S designed the experiments. Y.X.C, M.H.H, and L.W, fabricated materials and performed material characterizations. J.Y. performed FRAP analysis. S.Y. conducted confocal imaging and image analysis. Y.X.C performed cell culture. M.K. and J. L.O designed and performed the cancer-invasion experiments. All authors contributed to writing the paper.

References

[1] Tibbitt, M. W., and Anseth, K. S., 2009, "Hydrogels as Extracellular Matrix Mimics for 3D Cell Culture," Biotechnol. Bioeng., **103**(4), pp. 655–663.
[2] Hutmacher, D. W., Horch, R. E., Loessner, D., Rizzi, S., Sieh, S., Reichert, J. C., Clements, J. A., Beier, J. P., Arkudas, A., and Bleiziffer, O., 2009, "Translating Tissue Engineering Technology Platforms Into Cancer Research," J. Cell. Mol. Med., **13**(8a), pp. 1417–1427.
[3] Griffith, L. G., and Swartz, M. A., 2006, "Capturing Complex 3D Tissue Physiology In Vitro," Nat. Rev. Mol. Cell Biol., **7**(3), pp. 211–224.
[4] Albini, A., Iwamoto, Y., Kleinman, H., Martin, G., Aaronson, S., Kozlowski, J., and McEwan, R., 1987, "A Rapid In Vitro Assay for Quantitating the Invasive Potential of Tumor Cells," Cancer Res., **47**(12), pp. 3239–3245.
[5] Albini, A., and Benelli, R., 2007, "The Chemoinvasion Assay: A Method to Assess Tumor and Endothelial Cell Invasion and Its Modulation," Nat. Protocols, **2**(3), pp. 504–511.
[6] Marshall, J., 2011, "Transwell® Invasion Assays," *Cell Migration*, Springer, New York, pp. 97–110.
[7] Loessner, D., Stok, K. S., Lutolf, M. P., Hutmacher, D. W., Clements, J. A., and Rizzi, S. C., 2010, "Bioengineered 3D Platform to Explore Cell–ECM Interactions and Drug Resistance of Epithelial Ovarian Cancer Cells," Biomaterials, **31**(32), pp. 8494–8506.
[8] Schwartz, M. P., Fairbanks, B. D., Rogers, R. E., Rangarajan, R., Zaman, M. H., and Anseth, K. S., 2010, "A Synthetic Strategy for Mimicking the Extracellular Matrix Provides New Insight About Tumor Cell Migration," Integr. Biol., **2**(1), pp. 32–40.
[9] Artym, V. V., Yamada, K. M., and Mueller, S. C., 2009, "ECM Degradation Assays for Analyzing Local Cell Invasion," *Extracellular Matrix Protocols*, Springer, New York, pp. 211–219.
[10] Nyström, M., Thomas, G., Stone, M., Mackenzie, I., Hart, I., and Marshall, J., 2005, "Development of a Quantitative Method to Analyse Tumour Cell Invasion in Organotypic Culture," J. Pathol., **205**(4), pp. 468–475.
[11] Gill, B. J., Gibbons, D. L., Roudsari, L. C., Saik, J. E., Rizvi, Z. H., Roybal, J. D., Kurie, J. M., and West, J. L., 2012, "A Synthetic Matrix With Independently Tunable Biochemistry and Mechanical Properties to Study Epithelial Morphogenesis and EMT in a Lung Adenocarcinoma Model," Cancer Res., **72**(22), pp. 6013–6023.
[12] Huh, D., Hamilton, G. A., and Ingber, D. E., 2011, "From 3D Cell Culture to Organs-on-Chips," Trends Cell Biol., **21**(12), pp. 745–754.
[13] Minuth, W. W., Denk, L., and Glashauser, A., 2010, "A Modular Culture System for the Generation of Multiple Specialized Tissues," Biomaterials, **31**(11), pp. 2945–2954.
[14] Grinnell, F., 2000, "Fibroblast–Collagen–Matrix Contraction: Growth-Factor Signalling and Mechanical Loading," Trends Cell Biol., **10**(9), pp. 362–365.
[15] Bruggeman, L. A., Doan, R. P., Loftis, J., Darr, A., and Calabro, A., 2012, "A Cell Culture System for the Structure and Hydrogel Properties of Basement Membranes: Application to Capillary Walls," Cellular and Mol. Bioeng., **5**(2), pp. 194–204.
[16] Mohammadi, H., Janmey, P. A., and McCulloch, C. A., 2014, "Lateral Boundary Mechanosensing by Adherent Cells in a Collagen Gel System," Biomaterials, **35**(4), pp. 1138–1149.
[17] Gonen-Wadmany, M., Oss-Ronen, L., and Seliktar, D., 2007, "Protein–Polymer Conjugates for Forming Photopolymerizable Biomimetic Hydrogels for Tissue Engineering," Biomaterials, **28**(26), pp. 3876–3886.
[18] Nichol, J. W., Koshy, S. T., Bae, H., Hwang, C. M., Yamanlar, S., and Khademhosseini, A., 2010, "Cell-Laden Microengineered Gelatin Methacrylate Hydrogels," Biomaterials, **31**(21), pp. 5536–5544.
[19] Soman, P., Chung, P. H., Zhang, A. P., and Chen, S., 2013, "Digital Microfabrication of User-Defined 3D Microstructures in Cell-Laden Hydrogels," Biotechnol. Bioeng., **110**(11), pp. 3038–3047.
[20] Fairbanks, B. D., Singh, S. P., Bowman, C. N., and Anseth, K. S., 2011, "Photodegradable, Photoadaptable Hydrogels via Radical-Mediated Disulfide Fragmentation Reaction," Macromolecules, **44**(8), pp. 2444–2450.
[21] Brinkman, W. T., Nagapudi, K., Thomas, B. S., and Chaikof, E. L., 2003, "Photo-Cross-Linking of Type I Collagen Gels in the Presence of Smooth Muscle Cells: Mechanical Properties, Cell Viability, and Function," Biomacromolecules, **4**(4), pp. 890–895.
[22] Axelrod, D., Koppel, D., Schlessinger, J., Elson, E., and Webb, W., 1976, "Mobility Measurement by Analysis of Fluorescence Photobleaching Recovery Kinetics," Biophys. J., **16**(9), pp. 1055–1069.
[23] Leddy, H. A., and Guilak, F., 2003, "Site-Specific Molecular Diffusion in Articular Cartilage Measured Using Fluorescence Recovery After Photobleaching," Ann. Biomed. Eng., **31**(7), pp. 753–760.
[24] Lieleg, O., Baumgärtel, R. M., and Bausch, A. R., 2009, "Selective Filtering of Particles by the Extracellular Matrix: An Electrostatic Bandpass," Biophys. J., **97**(6), pp. 1569–1577.
[25] Lieleg, O., and Ribbeck, K., 2011, "Biological Hydrogels as Selective Diffusion Barriers," Trends Cell Biol., **21**(9), pp. 543–551.
[26] Nguyen, D. X., Bos, P. D., and Massague, J., 2009, "Metastasis: From Dissemination to Organ-Specific Colonization," Nat. Rev. Cancer, **9**(4), pp. 274–284.
[27] Cailleau, R., Young, R., Olive, M., and Reeves, W. J., Jr., 1974, "Breast Tumor Cell Lines From Pleural Effusions," J. Nat. Cancer Inst., **53**(3), pp. 661–674.
[28] Nicodemus, G. D., and Bryant, S. J., 2008, "Cell Encapsulation in Biodegradable Hydrogels for Tissue Engineering Applications," Tissue Eng. Part B Rev., **14**(2), pp. 149–165.
[29] Drury, J. L., and Mooney, D. J., 2003, "Hydrogels for Tissue Engineering: Scaffold Design Variables and Applications," Biomaterials, **24**(24), pp. 4337–4351.
[30] Hunt, N. C., and Grover, L. M., 2010, "Cell Encapsulation Using Biopolymer Gels for Regenerative Medicine," Biotechnol. Lett., **32**(6), pp. 733–742.

[31] Wirtz, D., Konstantopoulos, K., and Searson, P. C., 2011, "The Physics of Cancer: The Role of Physical Interactions and Mechanical Forces in Metastasis," Nat. Rev. Cancer, **11**(7), pp. 512–522.
[32] Gieni, R. S., and Hendzel, M. J., 2008, "Mechanotransduction From the ECM to the Genome: Are the Pieces Now in Place?," J. Cell. Biochem., **104**(6), pp. 1964–1987.
[33] Bott, K., Upton, Z., Schrobback, K., Ehrbar, M., Hubbell, J. A., Lutolf, M. P., and Rizzi, S. C., 2010, "The Effect of Matrix Characteristics on Fibroblast Proliferation in 3D Gels," Biomaterials, **31**(32), pp. 8454–8464.
[34] Even-Ram, S., and Yamada, K. M., 2005, "Cell Migration in 3D Matrix," Curr. Opin. Cell Biol., **17**(5), pp. 524–532.
[35] Janmey, P. A., and Miller, R. T., 2011, "Mechanisms of Mechanical Signaling in Development and Disease," J. Cell Sci., **124**(1), pp. 9–18.
[36] Burdick, J. A., and Anseth, K. S., 2002, "Photoencapsulation of Osteoblasts in Injectable RGD-Modified PEG Hydrogels for Bone Tissue Engineering," Biomaterials, **23**(22), pp. 4315–4323.
[37] Bryant, S. J., and Anseth, K. S., 2002, "Hydrogel Properties Influence ECM Production by Chondrocytes Photoencapsulated in Poly(Ethylene Glycol) Hydrogels," J. Biomed. Mater. Res., **59**(1), pp. 63–72.
[38] DeForest, C. A., and Anseth, K. S., 2012, "Advances in Bioactive Hydrogels to Probe and Direct Cell Fate," Ann. Rev. Chem. Biomol. Eng., **3**(1), pp. 421–444.